
Desingularization of Nonelementary Singularities

In this chapter we provide the basic tool for studying nonelementary singularities of a differential system in the plane. This tool is based on changes of variables called blow-ups. We use this technique for classifying the nilpotent singularities; i.e., the singularities having both eigenvalues zero but whose linear part is not identically zero. Blow-up is also used to show that at isolated singularities an analytic system has a finite sectorial decomposition.

3.1 Homogeneous Blow-Up

Before describing the effective algorithm that we use in the program P4 [9], and which is based on the use of quasihomogeneous blow-up, we will first explain the basic ideas only introducing *homogeneous blow-up*, which essentially means using polar coordinates. We position the singularity that we want to study at the origin.

Let 0 be a singularity of a C^∞ vector field X on \mathbb{R}^2 . Consider the map

$$\begin{aligned} \phi : \mathbb{S}^1 \times \mathbb{R} &\rightarrow \mathbb{R}^2 \\ (\theta, r) &\mapsto (r \cos \theta, r \sin \theta) . \end{aligned}$$

We can define a C^∞ vector field \hat{X} on the cylinder $\mathbb{S}^1 \times \mathbb{R}$ such that $\phi_*(\hat{X}) = X$, in the sense that $D\phi_v(\hat{X}(v)) = X(\phi(v))$. It is called the pull back of X by ϕ . It is nothing else but X written down in polar coordinates. The map ϕ is a C^∞ diffeomorphism, hence a genuine C^∞ coordinate change on $\mathbb{S}^1 \times (0, \infty)$, but not on $\{r = 0\}$; ϕ sends $\{r = 0\}$ to $(0, 0)$, and as such, the inverse mapping ϕ^{-1} blows up the origin to a circle. In order to study the phase portrait of X in a neighborhood V of the origin, it clearly suffices to study the phase portrait of \hat{X} on the neighborhood $\phi^{-1}(V)$ of the circle $\mathbb{S}^1 \times \{0\}$, and we can even restrict to $\{r \geq 0\}$. A priori this might seem a more difficult problem than the original one, but as we will see in this chapter, the construction is very helpful. If the k -jet $j_k(X)(0)$ is zero, then $j_k(\hat{X})(u) = 0$ for all $u \in \mathbb{S}^1 \times \{0\}$.

Although the cylinder is a good surface for getting a global view of \hat{X} and its phase portrait, it is often less appropriate for making calculations, since we constantly have to deal with trigonometric expressions. For that reason it is often preferable to make the calculations in different charts.

On the parts of the cylinder given, respectively, by $\theta \in (-\pi/2, \pi/2)$ and $\theta \in (\pi/2, 3\pi/2)$ use a chart given by

$$K^x : (\theta, r) \mapsto (r \cos \theta, \tan \theta) = (\bar{x}, \bar{y}).$$

In this chart the expression of the blow-up map ϕ is given by

$$\phi^x : (\bar{x}, \bar{y}) \mapsto (\bar{x}, \bar{x}\bar{y}). \quad (3.1)$$

Indeed we see that

$$\begin{aligned} \phi = \phi^x \circ K^x : (\theta, r) &\xrightarrow{K^x} (r \cos \theta, \tan \theta) \\ &\xrightarrow{\phi^x} (r \cos \theta, r \cos \theta \tan \theta) = (r \cos \theta, r \sin \theta). \end{aligned} \quad (3.2)$$

We call (3.1) a “blow-up in the x -direction”; the pull-back of X by means of ϕ^x is denoted by \hat{X}^x , i.e., $(\phi^x)_*(\hat{X}^x) = X$.

On the parts of the cylinder given, respectively, by $\theta \in (0, \pi)$ and $\theta \in (\pi, 2\pi)$, we use a chart given by

$$K^y : (\theta, r) \mapsto (\cot \theta, r \sin \theta) = (\bar{x}, \bar{y}).$$

In this chart the expression of the blow-up map ϕ is given by

$$\phi^y : (\bar{x}, \bar{y}) \mapsto (\bar{x}\bar{y}, \bar{y}), \quad (3.3)$$

in the sense that $\phi = \phi^y \circ K^y$. We call (3.3) a “blow-up in the y -direction”; the pullback of X by means of ϕ^y is denoted by \hat{X}^y , i.e., $(\phi^y)_*(\hat{X}^y) = X$.

Both ϕ^x and ϕ^y are called “directional blow-ups.”

If $j_k(X)(0) = 0$ and $j_{k+1}(X)(0) \neq 0$, then again $j_k(\hat{X}^x)(z) = 0$ and $j_k(\hat{X}^y)(z) = 0$ for, respectively, $z \in \{\bar{x} = 0\}$ or $z \in \{\bar{y} = 0\}$.

In case $j_k(X)(0) = 0$ and $j_{k+1}(X)(0) \neq 0$ the pullback \hat{X} and likewise \hat{X}^x and \hat{X}^y , are quite degenerate, and to make the situation less degenerate we consider \bar{X} with

$$\bar{X} = \frac{1}{r^k} \hat{X}.$$

Then \bar{X} also is a C^∞ vector field on $\mathbb{S}^1 \times \mathbb{R}$. On $\{r > 0\}$ this division does not change the orbits of \hat{X} or their sense of direction, but only the parametrization by t . From the formulas it is clear that singularities of $\bar{X}|_{\{r=0\}}$ come in pairs of opposite points.

For the related directional blow-up we use $(1/\bar{x}^k)\hat{X}^x$ in case (3.1) and $(1/\bar{y}^k)\hat{X}^y$ in case (3.3). On $\{\bar{x} \neq 0\}$ (respectively $\{\bar{y} \neq 0\}$) the vector fields

$(1/r^k)\hat{X}$ and $(1/\bar{x}^k)\hat{X}^x$ (respectively $(1/\bar{y}^k)\hat{X}^y$) are no longer equal up to analytic coordinate change, as were \hat{X} and \hat{X}^x (respectively, \hat{X}^y), but they are the same up to analytic coordinate change and multiplication by a nonzero analytic function.

We work this out for the blow-up in the x -direction: since $\phi = \phi^x \circ K^x$, we see that $(K^x)_*(\hat{X}) = \hat{X}^x$.

As such

$$(K^x)_*(\bar{X}) = (K^x)_*(\hat{X}/r^k) = \frac{1}{r^k}(K^x)_*(\hat{X}) = \frac{1}{r^k}\hat{X}^x = \bar{X}^x\left(\frac{\bar{x}}{r}\right)^k.$$

Seen in (θ, r) -coordinates we have $\bar{x}/r = \cos\theta$, which is strictly positive on the part of the cylinder given by $\theta \in (-\pi/2, \pi/2)$.

Similarly in the y -direction, we have $(K^y)_*(\hat{X}) = \hat{X}^y$ and $(K^y)_*(\bar{X}) = \bar{X}^y(\sin\theta)^k$, with $\sin\theta > 0$ on the part of the cylinder given by $\theta \in (0, \pi)$.

The directional blow-up ϕ^x can also be used for making a study on $\{(\theta, r) : \theta \in (\pi/2, 3\pi/2), r \geq 0\}$, but in that case we have $\cos\theta < 0$.

For odd k , this means that in the phase portraits that we find for $\bar{X}^x|_{\{\bar{x} \leq 0\}}$ we have to reverse time. A similar observation has to be made in using \bar{X}^y for studying \bar{X} on $\{(\theta, r) : \theta \in (\pi, 2\pi), r > 0\}$.

Such a time reversal could be avoided in using ϕ^x (respectively, ϕ^y) only for $\bar{x} \geq 0$ (respectively, $\bar{y} \geq 0$), and adding two extra directional blow-ups

$$\begin{aligned}\phi^{-x} : (\bar{x}, \bar{y}) &\mapsto (-\bar{x}, -\bar{x}\bar{y}), \\ \phi^{-y} : (\bar{x}, \bar{y}) &\mapsto (-\bar{x}\bar{y}, -\bar{y}),\end{aligned}$$

that we limit to, respectively, $\bar{x} \geq 0$ and $\bar{y} \geq 0$. Of course the number of calculations can be limited by using both ϕ^x and ϕ^y on a full neighborhood of, respectively, $\{\bar{x} = 0\}$ and $\{\bar{y} = 0\}$, avoiding having to work with ϕ^{-x} and ϕ^{-y} .

We now treat a few examples.

Example 3.1 First we present an example in which we use one blow-up to obtain quite easily the topological picture of the orbit structure of the singularity:

$$X = (x^2 - 2xy)\frac{\partial}{\partial x} + (y^2 - xy)\frac{\partial}{\partial y} + O(\|(x, y)\|^3).$$

The formulas for (polar) blow-up are

$$\bar{X} = \eta_1 \frac{\partial}{\partial \theta} + \eta_2 r \frac{\partial}{\partial r},$$

with

$$\begin{aligned}\eta_1(\theta, r) &= \frac{1}{r^{k+2}} \left\langle X, x \frac{\partial}{\partial y} - y \frac{\partial}{\partial x} \right\rangle (\phi(r, \theta)) \\ &= \frac{1}{r^{k+2}} (-r \sin \theta X_1(r \cos \theta, r \sin \theta) + r \cos \theta X_2(r \cos \theta, r \sin \theta)), \\ \eta_2(\theta, r) &= \frac{1}{r^{k+2}} \left\langle X, x \frac{\partial}{\partial x} + y \frac{\partial}{\partial y} \right\rangle (\phi(r, \theta)) \\ &= \frac{1}{r^{k+2}} (r \cos \theta X_1(r \cos \theta, r \sin \theta) + r \sin \theta X_2(r \cos \theta, r \sin \theta)),\end{aligned}$$

In our example $k = 1$ and the result is

$$\begin{aligned}\bar{X}(\theta, r) &= (\cos \theta \sin \theta (3 \sin \theta - 2 \cos \theta) + O(r)) \frac{\partial}{\partial \theta} \\ &\quad + r(\cos^3 \theta - 2 \cos^2 \theta \sin \theta - \cos \theta \sin^2 \theta + \sin^3 \theta + O(r)) \frac{\partial}{\partial r}.\end{aligned}$$

Zeros on $\{r = 0\}$ are located at

$$\theta = 0, \pi; \theta = \pi/2, 3\pi/2; \tan \theta = 2/3.$$

At these singularities, the radial eigenvalue is given by the coefficient of $r\partial/\partial r$ while the tangential eigenvalue can be found by differentiating the $\partial/\partial\theta$ -component with respect to θ . One thus obtains Fig. 3.1. In this figure we represent the half cylinder $S^1 \times [0, \infty)$ as $E = \{(x, y) : x^2 + y^2 \geq 1\}$. This visualization will also be used in the sequel. The phase portrait which we see on E near the circle $C = \{x^2 + y^2 = 1\}$ gives a very good idea of the phase portrait of X near the origin. It suffices to shrink the circle to a point (see Fig. 3.2).

All the singularities on $S^1 \times \{0\}$ are hyperbolic. We say that we have desingularized X at 0 since all singularities of $\bar{X}|_{\{r=0\}}$ are elementary. The

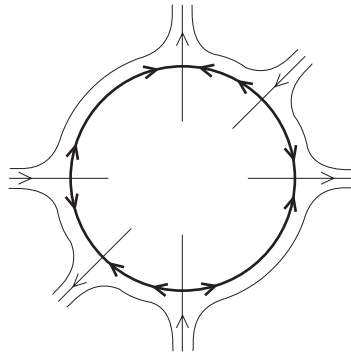


Fig. 3.1. Blow-up of Example 3.1

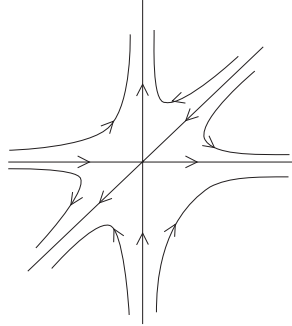


Fig. 3.2. Local phase portrait of Example 3.1

exact value of the eigenvalues at the different singularities depends only on the 2-jet of X . Using techniques similar to the ones that served to study the C^0 -conjugacy classes of elementary singularities, one can now prove that X near the origin is C^0 -conjugate to the vector field $Y = j_2X(0)$, which has a similar blow-up. We will not work this out. In this chapter we will only take care of determining the sectorial decomposition of the singularity. Although in the line of what we did explicitly for the elementary singularities, it is rather tedious to show that for each kind of sectorial decomposition of an analytic vector field there only exists one model for C^0 -conjugacy. We refer to [53] or [33] for a detailed elaboration. The proof on the unicity of the model for C^0 -equivalence is simpler, but nevertheless we do not wish to pay attention to such constructions in general. We will treat some specific situations in the exercises.

Concerning the sectorial decomposition, we remark that in the case of the example, it is not hard to show, using the blow-up, that the vector field X indeed has a finite sectorial decomposition near 0 as defined in Sect. 1.5. We will come back to the proof of this in Sect. 3.5.

Concerning Fig. 3.1, we remark that the exact position of the invariant manifolds, transverse to C , of the six hyperbolic singularities in the blow-up can be approximated by Taylor approximation. After blowing down it leads to an accurate presentation of the six “separatrices” in the local phase portrait; see Fig. 3.2. □

Example 3.2 Second we present an example for which blowing up once is not sufficient to desingularize the singularity. There remain nonelementary singularities of $\bar{X}|_{\{r=0\}}$ at which we need to repeat the blow-up construction, leading to successive blowing up. The starting vector field is

$$y \frac{\partial}{\partial x} + (x^2 + xy) \frac{\partial}{\partial y} + O(\|(x, y)\|^3).$$

Blowing up in the y -direction gives no singularities on $\{\bar{y} = 0\}$. Direct calculations show that the singularities of \bar{X} (and equally for \bar{X}^x and \bar{X}^y),

as well as their eigenvalues, depend only on the first nonzero jet, hence on $y\partial/\partial x$ in this example. We now perform a blow-up in the x -direction, working out the calculations explicitly. Writing

$$x = \bar{x}, \quad y = \bar{x}\bar{y},$$

or

$$\bar{x} = x, \quad \bar{y} = y/x,$$

we get

$$\begin{aligned} \dot{\bar{x}} &= \dot{x} \\ &= y + O(\|(x, y)\|^3) \\ &= \bar{y}\bar{x} + O(|\bar{x}|^3), \\ \dot{\bar{y}} &= \frac{\dot{y}}{x} - y\frac{\dot{x}}{x^2} \\ &= (x + y) + \frac{1}{x}O(\|(x, y)\|^3) - \frac{y^2}{x^2} - \frac{y}{x^2}O(\|(x, y)\|^3) \\ &= \bar{x} + \bar{y}\bar{x} - \bar{y}^2 + O(|\bar{x}|^2). \end{aligned} \tag{3.4}$$

The only singularity on $\bar{x} = 0$ occurs for $\bar{y} = 0$, where the 1-jet of the vector field \bar{X}^x at this singularity is $\bar{x}\partial/\partial\bar{y}$.

As the singularity is nonelementary, we are going to perform an extra blow-up in order to study it. Blowing up in the \bar{x} -direction gives no singularities. Blowing up (3.4) in the \bar{y} -direction ($\bar{x} = \bar{y}\bar{\bar{x}}, \bar{y} = \bar{y}$) gives

$$\begin{aligned} \dot{\bar{\bar{y}}} &= \dot{\bar{y}} \\ &= (\bar{x} + \bar{y}\bar{x} - \bar{y}^2 + O(|\bar{x}|^2)) \\ &= \bar{\bar{x}}\bar{y} - \bar{y}^2 + O(\|(\bar{\bar{x}}, \bar{y})\|^3), \\ \dot{\bar{\bar{x}}} &= \frac{\dot{\bar{x}}}{\bar{y}} - \bar{x}\frac{\dot{\bar{y}}}{\bar{y}^2} \\ &= \bar{x} + \frac{1}{\bar{y}}O(|\bar{x}|^3) - \frac{\bar{x}}{\bar{y}^2}(\bar{x} + \bar{y}\bar{x} - \bar{y}^2 + O(|\bar{x}|^2)) \\ &= \bar{\bar{y}}\bar{\bar{x}} - \bar{\bar{x}}^2 + \bar{\bar{y}}\bar{\bar{x}} + O(\|(\bar{\bar{x}}, \bar{\bar{y}})\|^2). \end{aligned}$$

The 2-jet is now $(\bar{\bar{x}}\bar{\bar{y}} - \bar{\bar{y}}^2)\partial/\partial\bar{\bar{y}} + (2\bar{\bar{x}}\bar{\bar{y}} - \bar{\bar{x}}^2)\partial/\partial\bar{\bar{x}}$. This singularity is not elementary, but as we have seen in Example 3.1, it can be studied by blowing up once. This succession of blowing up is schematized in Fig. 3.3. At each step we blow-up a point to a circle, not forgetting that singularities of \bar{X} on $\{r = 0\}$ always come in pairs of opposite points. If we need to blow-up one, we also apply the same blow-up procedure to the second. As we already observed in discussing the directional blow-up \bar{X}^x and \bar{X}^y in relation to \bar{X} , the study of both singularities at a pair of opposite points can be done on the same expressions by treating $\bar{x} \leq 0$ as well as $\bar{x} \geq 0$, or, respectively, $\bar{y} \leq 0$ as well

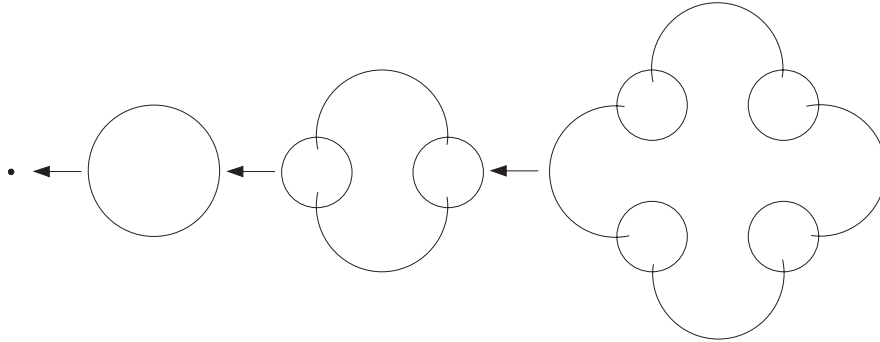


Fig. 3.3. Successive blowing up

as $\bar{y} \geq 0$. In terms of \bar{X} it also means that we only have to consider one of the singularities, but considering $r \leq 0$ as well as $r \geq 0$. It is possible that we have to use a time-reversal, when k is odd (with $\bar{X} = \hat{X}/r^k$), when transporting information to the other singularity. At each step of the succession of blow-ups we only need to keep part of the information, sufficient to cover a full neighborhood of the origin after blowing down.

This procedure of successive blowing up can be formalized as follows, providing an overall geometric view like in Fig. 3.3. Instead of using the polar blow-up ϕ and dividing by some power of r , we use the map

$$\tilde{\phi} : \left\{ z \in \mathbb{R}^2 : \|z\| > \frac{1}{2} \right\} \subset \mathbb{R}^2 \rightarrow \mathbb{R}^2, z \mapsto z - \frac{z}{\|z\|},$$

and divide by the same power of $(\|z\| - 1)$.

The vector field we so obtain is analytically equivalent to \bar{X} , but the second is now defined on an open domain in \mathbb{R}^2 and therefore it becomes easier to visualize how we can blow-up again at some point $z_0 \in \{z \in \mathbb{R}^2 : \|z\| = 1\}$: we just use the mapping $T_{z_0} \circ \phi$ where T_{z_0} denotes the translation $z \mapsto z + z_0$.

As we again end up on an open domain of \mathbb{R}^2 we can repeat the construction if necessary. For simplicity in notation we denote the first blow-up by ϕ_1 , the second by ϕ_2 and so on.

After a sequence of n blow-ups we find some C^∞ -vector field \bar{X}^n defined on a domain $U_n \subset \mathbb{R}^2$. \bar{X}^n is even analytic if we start with an analytic X . We write $\Gamma_n = (\phi_1 \circ \dots \circ \phi_n)^{-1}(0) \subset U_n$. Only one of the connected components of $\mathbb{R}^2 \setminus \Gamma_n$, call it A_n , has a noncompact closure. Furthermore $\partial A_n \subset \Gamma_n$ and ∂A_n , which is homeomorphic to \mathbb{S}^1 consists of a finite number of analytic regular closed arcs meeting transversely. The mapping $(\phi_1 \circ \dots \circ \phi_n)|_{A_n}$ is an analytic diffeomorphism sending A_n onto $\mathbb{R}^2 \setminus \{0\}$. There exists a strictly positive function F_n on A_n such that $\hat{X}^n = F_n \bar{X}^n$ and $\hat{X}^n|_{A_n}$ is analytically diffeomorphic to $X|_{\mathbb{R}^2 \setminus \{0\}}$ by means of the diffeomorphism $(\phi_1 \circ \dots \circ \phi_n)|_{A_n}$. The function F_n extends in a C^ω way to ∂A_n where in general it is 0.

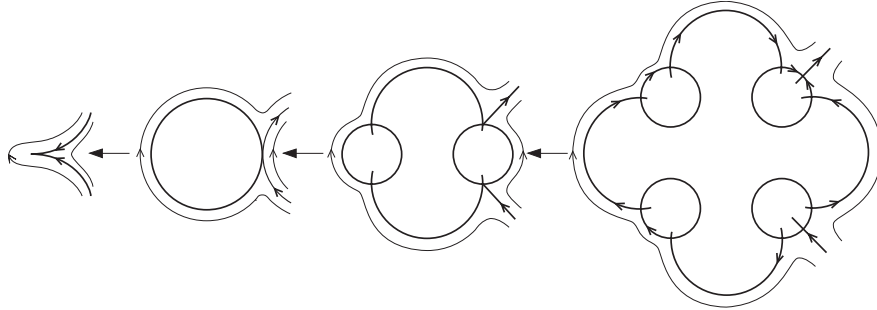


Fig. 3.4. Blowing up Example 3.2

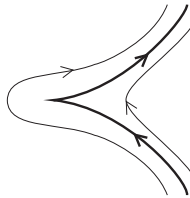


Fig. 3.5. Local phase portrait of Example 3.2

The reconstruction of the local phase portrait of Example 3.2 is represented in Fig. 3.4. To understand the figure one has to start from the right, representing the phase portrait of a vector field \bar{X}^3 obtained after three blow-ups. One must not forget that at the second step one simultaneously blows up two (opposite) singularities and at the third step their 4 counter images. The calculations show that all the singularities of \bar{X}^3 on ∂A_3 are hyperbolic, and hence, that \bar{X}^3 is a desingularization of X . We say that X has been desingularized after three successive blow-ups. The structure of the desingularization of \bar{X}^3 is as represented in Fig. 3.4. In following the arrows to the left, we successively represent the phase portraits of \bar{X}^2 near ∂A_2 , \bar{X}^1 near ∂A_1 , and finally X near the origin. The sectorial decomposition of X near the origin is clear from its desingularization \bar{X}^3 .

Again the method permits us to show that the vector fields of Example 3.2 are topologically determined by the 2-jet in the sense that such X near 0 is C^0 -conjugate to $Y = j_2 X(0)$. A precise drawing of the two separatrices of the *cusp* can be obtained by using Taylor approximations of the invariant manifolds in the desingularization followed by a blowing down, as shown in Fig. 3.5. □

3.2 Desingularization and the Łojasiewicz Property

To control whether a sequence of blow-ups finally leads to a desingularization we use the notion of a *Łojasiewicz inequality*. We say that a vector field X on

\mathbb{R}^2 satisfies a Lojasiewicz inequality at 0 if there is a $k \in \mathbb{N}$ with $k \geq 1$, and a $c > 0$ such that $\|X(x)\| \geq c\|x\|^k$ on some neighborhood of 0.

For analytic vector fields at isolated singularities, a Lojasiewicz inequality always holds (see [18]).

Theorem 3.3 ([52]) *If X at 0 satisfies a Lojasiewicz inequality, then there exists a finite sequence of blowing ups $\phi_1 \circ \dots \circ \phi_n$ leading to a vector field \bar{X}^n defined in the neighborhood of ∂A_n of which the singularities on ∂A_n are elementary.*

These elementary singularities can be as follows:

- (i) *Isolated singularities p which are hyperbolic or semi-hyperbolic with non-flat behavior on the center manifold;*
- (ii) *Regular analytic closed curves (or possibly the whole of ∂A_n when $n = 1$) along which \bar{X}^n is normally hyperbolic.*

The position on ∂A_n as well as the determining properties of the singularities as used in the classification presented in the Theorems 2.15 and 2.19 depend only on a finite jet of X .

We do not give a proof of this theorem. We merely consider blow-up as a technique to desingularize singularities. The technique turns out to be successful, at least if we apply it to a singularity of Lojasiewicz type, such as an isolated singularity of an analytic system.

Taking a close look at the singularities of \bar{X}^n on ∂A_n , we see that some lie on regular arcs of ∂A_n , while others lie in corners. At the former we see, because of the Theorems 2.15 and 2.19, that there always exists an invariant C^∞ curve, transversely cutting ∂A_n , unless the singularity is a resonant hyperbolic node. The most degenerate one is such that the linear part of the singularity consists of a single Jordan block. We represent the attracting case in Fig. 3.6a. In any case, near all singularities on the regular part of ∂A_n we find at least one orbit that blows down to a characteristic orbit of X . We repeat, from Sect. 1.6, that a characteristic orbit is an orbit which tends to the singularity, either in positive or negative time, with a well-defined slope. We see therefore that X necessarily has a characteristic orbit at 0 if \bar{X}^n has at least one singularity on the regular parts of ∂A_n .

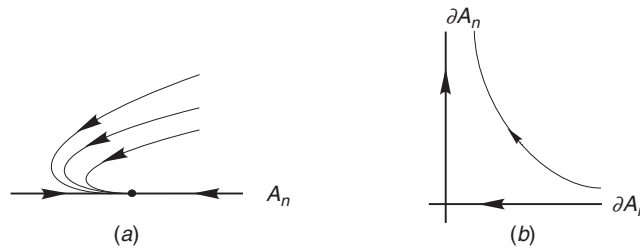


Fig. 3.6. Some singularities of \bar{X} on ∂A_n

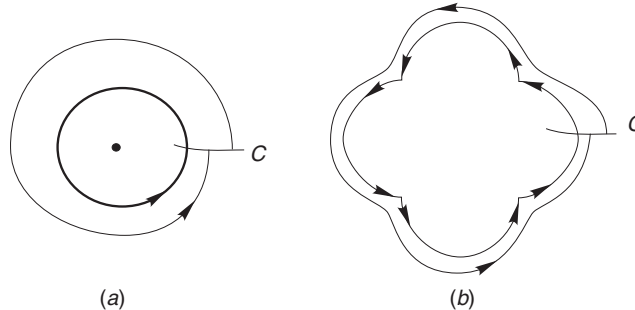


Fig. 3.7. Samples of desingularizations of monodromic orbits

Singularities at corners of ∂A_n also lead to the existence of characteristic orbits, except when the singularity has a hyperbolic sector with both separatrices in A_n , as represented in Fig. 3.6b.

Because of Theorem 3.3, and the observation just made, we thus see that a Lojasiewicz singularity either has a characteristic orbit or, if it does not have a characteristic orbit, is a center or a focus. The latter situation is also called *monodromic*. This can only happen if either $\overline{X} = \overline{X}^1$ has no singularities on ∂A_1 (see Fig. 3.7a) or if all singularities are corners of saddle type (see Fig. 3.7b). In that case there is a segment C lying in $A_n \cup \partial A_n$ that is transverse to the flow of \overline{X} and cuts ∂A_n transversely at a regular point p . A first return map can be defined for values $q \in C$ for q sufficiently close to p .

We now treat the two cases separately, starting with the monodromic one. We consider only analytic systems, and we choose C to be an analytic curve with an analytic choice of a regular parameter s on it; we let $s = 0$ coincide with ∂A_n and $s > 0$ with A_n . In case there are no singularities (see Fig. 3.7a) the return map f is analytic in s , and as such, either $f(s) = s$ or $j_n(f(s) - s) \neq 0$ for some $n \in \mathbb{N}$ with $n \geq 1$. In the former case, \overline{X} represents a center, and in the latter case a focus. The focus need not to be a hyperbolic one, but is at least C^0 -conjugate to a hyperbolic focus.

In the case there are singularities (see Fig. 3.7b), then we enter into a really difficult subject. Although \overline{X} as well as \overline{X}^n are analytic, the first return map f does not need to be analytic. Nevertheless it is possible to prove that in this case as well the system is either a center or a focus, excluding the possibility of having accumulation of limit cycles at the singularities (which can occur in the C^∞ case).

An important paper dealing with the proof is [51]. The paper contains valuable results on which subsequent work still relies. It does not however provide a complete proof, leaving a gap that was detected only in the mid-seventies. For a while this gap was called Dulac's problem (see e.g., [113]). In the meantime the proof has been completed independently by Ecalle [59] and Ilyashenko [88].

In the case that characteristic orbits occur, we show how to prove that such singularities have a “finite sectorial decomposition” as defined in Sect. 1.6. We do not have to restrict to analytic systems, but can consider C^∞ singularities of Lojasiewicz type. The proof relies completely on Theorem 3.3, together with Theorems 2.15 and 2.19; we provide only a rough sketch, referring to the exercises for working out some of the details.

Choosing an orientation for ∂A_n we get a cyclic order on the singularities of $\overline{X^n}|_{\partial A_n}$. To fix the ideas, we suppose that ∂A_n is oriented in a clockwise way. We denote the cyclic order by “ $<$.” The only way to get a hyperbolic sector is by having two singularities p and q , neither lying in a corner of ∂A_n , such that:

- (i) Every singularity r with $p < r < q$ is a corner of saddle type;
- (ii) There is an invariant C^∞ curve C_1 (respectively, C_2), transversely cutting ∂A_n at p (respectively, q), which, together with $\partial A_n \cap [p, q]$ borders a hyperbolic sector.

For a general picture we refer to Fig. 3.8.

Based on the normal form given in the Theorems 2.15 and 2.19, it is an easy exercise to prove the existence of a C^∞ curve that transversely cuts both C_1 and C_2 and that meets, inside the hyperbolic sector in between C_1 and C_2 , the requirements expressed in the definition of “finite sectorial decomposition.”

The way to encounter an elliptic sector is by having two singularities p and q such that:

- (i) Every singularity r with $p < r < q$ is a corner of saddle type;
- (ii) Both at p and q there is a parabolic sector adherent to $[p, q] \subset \partial A_n$,

of which one is attracting and the other is repelling. We refer to Fig. 3.9 for an example. In this picture we cannot however guarantee that we see the full elliptic sector, and surely not the maximal one as defined in Sect. 1.5.

In fact the curve C_1 in Fig. 3.9 could be transverse to ∂A_n , but it could also belong to ∂A_n . It is also possible that C_2 (or its blow down) is not a good

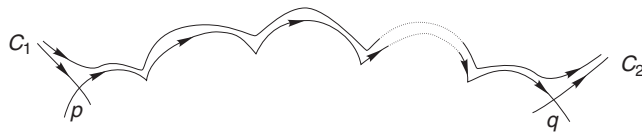


Fig. 3.8. Blowing up a hyperbolic sector

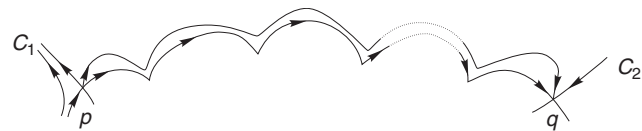


Fig. 3.9. Blowing up an elliptic sector

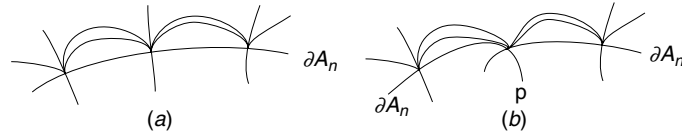


Fig. 3.10. Blowing up of part of adjacent elliptic sectors

choice for bordering a maximal elliptic sector, since it is possible that the orbits to the right of C_2 also tend in negative time to ∂A_n , and as such, belong to the elliptic sector if we want it to be maximal (in the sense that it is an elliptic sector of a minimal sectorial decomposition). From the desingularized vector field \overline{X}^n it is easy to find a maximal elliptic sector containing the part near $[p, q]$ as given in Fig. 3.9. We will treat some examples in the exercises.

We find two kind of bordering curves for a maximal elliptic sector. On the one hand there are the bordering curves which also border a hyperbolic sector. On the other hand there are bordering curves separating two adjacent elliptic sectors; their choice is not unique, as we see in the examples given in Fig. 3.10.

In any case, for an elliptic sector, the normal forms from the Theorems 2.15 and 2.19 permit us an easy proof of the existence of a C^∞ curve, transversely cutting the bordering curves and having the exact properties as described in the definition of “finite sectorial decomposition” (see Sect. 1.5).

In between two hyperbolic sectors one can encounter a unique maximal parabolic sector, whose desingularization can be quite complicated; however, based on the normal forms in the Theorems 2.15 and 2.19 one can easily find, inside any a priori chosen neighborhood of 0, a C^∞ curve, the portion of which that lies inside the parabolic sector is everywhere transverse to the orbits, including the bordering orbits. We again refer to the exercises for the details of the construction.

For a minimal sectorial decomposition it is always possible to find bordering curves or separatrices (see Sect. 1.5) which are images by a blow down mapping of a C^∞ curve. The ones bordering a hyperbolic sector are of *finite type* in the sense that they possess a C^∞ parametrization $\gamma : [0, \varepsilon] \mapsto \mathbb{R}^2$ with $j_r \gamma(0) \neq 0$ for some $r \in \mathbb{N}$. They can also be seen as graphs of a C^∞ function in the variable $x^{1/n}$ for some $n \in \mathbb{N}$ with $n \geq 1$ in suitable C^∞ coordinates (x, y) ; see [57]. The separatrices between two elliptic sectors do not need to have this property, which is the case for example in Fig. 3.10b if the corner point p is a semi-hyperbolic point. For more information see [57].

3.3 Quasihomogeneous blow-up

Although the method of successive homogeneous blow-ups is sufficient for studying isolated singularities of an analytic vector field, it turns out to be

much more efficient to include *quasihomogeneous blow-ups*. In fact the algorithm that we have implemented in the program P4 [9] relies on the systematic approach presented in [124], and which is based on the use of quasihomogeneous blow-ups; see also [23] and [22]. We first present the technique before describing the algorithm.

Let 0 be a singularity of a C^∞ vector field X on \mathbb{R}^2 . Consider the map

$$\begin{aligned} \phi : \mathbb{S}^1 \times \mathbb{R} &\rightarrow \mathbb{R}^2 \\ (\theta, r) &\mapsto (r^\alpha \cos \theta, r^\beta \sin \theta), \end{aligned}$$

for some well chosen $(\alpha, \beta) \in \mathbb{N} \times \mathbb{N}$ with $\alpha, \beta \geq 1$. Exactly as in the “homogeneous case,” where $(\alpha, \beta) = (1, 1)$, we can define a C^∞ vector field \hat{X} on $\mathbb{S}^1 \times \mathbb{R}$ with $\phi_*(\hat{X}) = X$. We will divide it by r^k , for some $k \in \mathbb{N}$ with $k \geq 1$, in order to get a C^∞ vector field $\bar{X} = \frac{1}{r^k} \hat{X}$, which is as non-degenerate as possible along the invariant circle $\mathbb{S}^1 \times \{0\}$.

In practice one again uses directional blow-ups:

$$\begin{aligned} \text{positive } x\text{-direction: } (\bar{x}, \bar{y}) &\mapsto (\bar{x}^\alpha, \bar{x}^\beta \bar{y}), \quad \text{leading to } \hat{X}_+^x, \\ \text{negative } x\text{-direction: } (\bar{x}, \bar{y}) &\mapsto (-\bar{x}^\alpha, \bar{x}^\beta \bar{y}), \quad \text{leading to } \hat{X}_-^x, \\ \text{positive } y\text{-direction: } (\bar{x}, \bar{y}) &\mapsto (\bar{x} \bar{y}^\alpha, \bar{y}^\beta), \quad \text{leading to } \hat{X}_+^y, \\ \text{negative } y\text{-direction: } (\bar{x}, \bar{y}) &\mapsto (\bar{x} \bar{y}^\alpha, -\bar{y}^\beta), \quad \text{leading to } \hat{X}_-^y, \end{aligned}$$

inducing also the systems \bar{X}_-^x , \bar{X}_+^x , \bar{X}_-^y and \bar{X}_+^y that we obtain dividing, respectively, by \bar{x}^k and \bar{y}^k .

If α is odd (respectively, β is odd), the information found in the positive x -direction (respectively, y -direction) also covers the one in the negative x -direction (respectively, y -direction).

To show by an example that this technique can be quite efficient, we again study the cusp-singularity

$$y \frac{\partial}{\partial x} + (x^2 + xy) \frac{\partial}{\partial y} + O(\|(x, y)\|^3), \quad (3.5)$$

this time using a quasihomogeneous blowing up with $(\alpha, \beta) = (2, 3)$.

In the positive x -direction we consider the transformation $(x, y) = (\bar{x}^2, \bar{x}^3 \bar{y})$. In this case we have $\dot{x} = 2\bar{x}\dot{\bar{x}}$, hence $\dot{\bar{x}} = \frac{1}{2}\bar{x}^2\dot{\bar{y}} + O(\bar{x}^3)$ and $\dot{y} = 3\bar{x}^2\dot{\bar{y}}\bar{x} + \bar{x}^3\dot{\bar{y}}$, hence $\dot{\bar{y}} = (1 - \frac{3}{2}\bar{y}^2)\bar{x} + O(\bar{x}^2)$. We divide by \bar{x} and find

$$\begin{aligned} \dot{\bar{x}} &= \frac{\bar{x}\dot{\bar{y}}}{2} + O(\bar{x}^2), \\ \dot{\bar{y}} &= 1 - \frac{3}{2}\bar{y}^2 + O(\bar{x}). \end{aligned}$$

We find two hyperbolic singularities of saddle type, situated at the points $(\bar{x}, \bar{y}) = (0, \pm\sqrt{2/3})$.

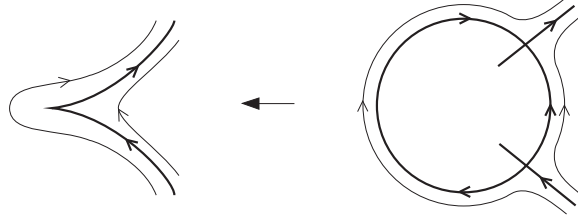


Fig. 3.11. Quasihomogeneous blow-up of the cusp singularity

Similar calculations in the negative \bar{x} -direction, as well as in the \bar{y} -direction show that no other singularities are present.

As such blowing up once suffices to desingularize the singularity leading to the picture in Fig. 3.11.

Again an accurate positioning of the invariant separatrices can be obtained by Taylor approximation of the stable and unstable manifolds.

A question one might ask is how to effectively find the coefficient (α, β) to use in a quasihomogeneous blow-up. This can be obtained by using the so called Newton diagram. We first define the Newton diagram.

Let $X = P(x, y)\frac{\partial}{\partial x} + Q(x, y)\frac{\partial}{\partial y}$ be a polynomial vector field with an isolated singularity at the origin.

Let $P(x, y) = \sum_{i+j \geq 1} a_{ij}x^i y^j$ and $Q(x, y) = \sum_{i+j \geq 1} b_{ij}x^i y^j$. The *support* of X is defined to be

$$S = \{(i - 1, j) : a_{ij} \neq 0\} \cup \{(i, j - 1) : b_{ij} \neq 0\} \subset \mathbb{R}^2,$$

and the *Newton polygon* of X is the convex hull Γ of the set

$$P = \bigcup_{(r,s) \in S} \{(r', s') : r' \geq r, s' \geq s\}.$$

The *Newton diagram* of X is the union γ of the compact faces γ_k of the Newton polygon Γ , which we enumerate from the left to the right. If there exists a face γ_k which lies completely on the half-plane $\{r \leq 0\}$, then we start the enumeration with $k = 0$, otherwise we start with $k = 1$. Since the origin is an isolated singularity we have that at least one of the points $(-1, s)$ or $(0, s)$ is an element of S for some s , and also at least one of the points $(r, 0)$ or $(r, -1)$ is an element of S for some r . Hence there always exists a face γ_1 in the Newton diagram.

Suppose that γ_1 has equation $\alpha r + \beta s = d$, with $\gcd(\alpha, \beta) = 1$. As a first step in the desingularization process we use a quasihomogeneous blow-up of degree (α, β) . As an example we calculate the Newton diagram of the vector field (3.5), providing the best choice of coefficients (α, β) .

The support of (3.5) surely contains $(-1, 1)$, $(2, -1)$, and $(1, 0)$ coming, respectively, from $y\frac{\partial}{\partial x}$, $x^2\frac{\partial}{\partial y}$, and $xy\frac{\partial}{\partial y}$. Besides these three points it can contain many other points, which are in fact not essential since they all lie

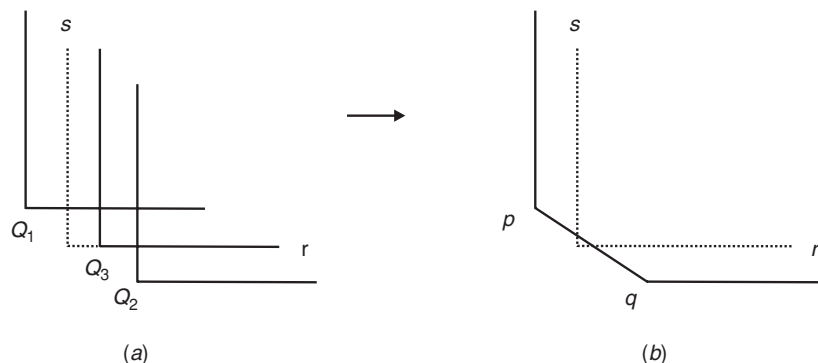


Fig. 3.12. Calculating the Newton polygon

in the convex hull Q of $Q_1 \cup Q_2 \cup Q_3$ with $Q_1 = \{(r, s) : r \geq -1, s \geq 1\}$, $Q_2 = \{(r, s) : r \geq 2, s \geq -1\}$, and $Q_3 = \{(r, s) : r \geq 1, s \geq 0\}$. In Fig. 3.12 we represent Q_i for $i = 1, 2, 3$ in (a) as well as $P = Q$ in (b).

We see that the Newton diagram consists of one compact face, that we denote by γ_1 and which is the line segment joining the points $p = (-1, 1)$ to $q = (2, -1)$. The line segment lies on the line of equation $2r + 3s = 1$ inducing the choice $(\alpha, \beta) = (2, 3)$.

In view of an efficient use of a quasihomogeneous blow-up with coefficients (α, β) we will no longer decompose a vector field in homogeneous components, but in adapted quasihomogeneous components. Based on this decomposition we will now describe an algorithm for blowing up.

We write

$$X = \sum_{j \geq d} X_j, \text{ where } X_j = P_j(x, y) \frac{\partial}{\partial x} + Q_j(x, y) \frac{\partial}{\partial y}$$

is the *quasihomogeneous component* of X of type (α, β) and quasihomogeneous degree j , that is to say $P_j(r^\alpha x, r^\beta y) = r^{j+\alpha} P_j(x, y)$ and $Q_j(r^\alpha x, r^\beta y) = r^{j+\beta} Q_j(x, y)$. After blowing up we will divide by r^d . In practice we first blow-up the vector field in the positive x -direction, yielding, after multiplying the result with $\alpha \bar{x}^{-d}$:

$$\begin{aligned} \dot{\bar{x}} &= \sum_{\delta \geq d} \bar{x}^{\delta+1-d} P_\delta(1, \bar{y}), \\ \bar{X}_+^x : \dot{\bar{y}} &= \sum_{\delta \geq d} \bar{x}^{\delta-d} (\alpha Q_\delta(1, \bar{y}) - \beta \bar{y} P_\delta(1, \bar{y})). \end{aligned}$$

We determine the singularities on the line $\{\bar{x} = 0\}$.

(1) If $\alpha Q_d(1, \bar{y}) - \beta \bar{y} P_d(1, \bar{y}) \neq 0$, the points $(0, \bar{y}_0)$ satisfying the equation $\alpha Q_d(1, \bar{y}) - \beta \bar{y} P_d(1, \bar{y}) = 0$ are isolated singularities of \bar{X} on the line $\{\bar{x} = 0\}$, at which

$$d(\bar{X}_+^x)_{(0, \bar{y}_0)} = \begin{pmatrix} P_d(1, \bar{y}_0) & 0 \\ \star & \alpha \frac{\partial Q_d}{\partial \bar{y}}(1, \bar{y}_0) - \beta (P_d(1, \bar{y}_0) + \bar{y}_0 \frac{\partial P_d}{\partial \bar{y}}(1, \bar{y}_0)) \end{pmatrix},$$

which immediately gives the eigenvalues as the diagonal entries. If the singularity is hyperbolic, we are done. If the singularity is semi-hyperbolic, we have to determine the behavior on the center manifold. If the singularity is nonelementary, we introduce $\tilde{y} = \bar{y} - \bar{y}_0$, and blow-up this vector field again in the positive \bar{x} -direction as well as in the positive and negative \tilde{y} -direction with a certain degree (α', β') , which we determine from the Newton diagram associated to the vector field.

(2) If $\alpha Q_d(1, \bar{y}) - \beta \bar{y} P_d(1, \bar{y}) \equiv 0$, we have a line of singularities. Since

$$D(\bar{X}_+^x)_{(0, \bar{y}_0)} = \begin{pmatrix} P_d(1, \bar{y}_0) & 0 \\ \star & 0 \end{pmatrix},$$

all the singularities are semi-hyperbolic, except those singularities $(0, \bar{y}_0)$ for which $P_d(1, \bar{y}_0) = 0$. The latter will require further blow-up.

Next we blow-up the vector field in the negative x -direction and study this vector field in the same way as in the previous case.

Finally we have to blow-up the vector field in the positive and the negative y -direction, and determine whether or not $(0, 0)$ is a singular point, since the others have been studied in the previous charts.

It is easy to see that $(0, 0)$ is a singularity if and only if γ_1 lies completely in the half-plane $\{r \geq 0\}$. If this is the case then $(0, 0)$ is elementary. Indeed, blowing up the vector field in the positive y -direction yields, after multiplying the result by $\beta \bar{y}^{-d}$:

$$\begin{aligned} \dot{\bar{x}} &= \sum_{\delta \geq d} \bar{y}^{\delta-d} (\beta P_\delta(\bar{x}, 1) - \alpha \bar{x} Q_\delta(\bar{x}, 1)), \\ \bar{X}_+^y : \dot{\bar{y}} &= \sum_{\delta \geq d} \bar{y}^{\delta+1-d} Q_\delta(\bar{x}, 1). \end{aligned}$$

Hence $(0, 0)$ is a singular point if $P_d(0, 1) = 0$, i.e., if $P_d(x, y) = xF(x, y)$, implying that γ_1 lies completely in the half-plane $\{r \geq 0\}$. Suppose now that $(0, 0)$ is a singular point of \bar{X}_+^y ; then we have

$$D(\bar{X}_+^y)_{(0,0)} = \begin{pmatrix} \beta \frac{\partial P_d}{\partial \bar{x}}(0, 1) - \alpha Q_d(0, 1) & \star \\ 0 & Q_d(0, 1) \end{pmatrix}.$$

Let $(0, s)$ be the intersection of the line γ_1 and the line $r = 0$. Then $P_d(x, y) = axy^s + G(x, y)$ and $Q_d(x, y) = by^{s+1} + H(x, y)$, with $a^2 + b^2 \neq 0$, $\deg_x G(x, y) \geq 2$ and $\deg_x H(x, y) \geq 1$. Hence $\beta \frac{\partial P_d}{\partial \bar{x}}(0, 1) - \alpha Q_d(0, 1) = a\beta - b\alpha$. So if $a\beta - b\alpha \neq 0$ then $(0, 0)$ is nonelementary. If $a\beta - b\alpha = 0$, then $Q_d(0, 1) = b \neq 0$, and $(0, 0)$ is elementary, too.

In [124] it has been proven that the algorithm, as presented here, leads to a desingularization. It is also more efficient than the usual one.

In the program P4 [9] we not only perform a detailed study near the singular points in \mathbb{R}^2 , but also near singular points at infinity. In Chap. 5 we will describe how polynomial vector fields on \mathbb{R}^2 can be extended to infinity. We now apply the blow-up technique to study nilpotent singularities.

3.4 Nilpotent Singularities

In this section we study singularities, positioned at the origin, at which the linear approximation $DX(0)$ of the vector field X is linearly conjugate to $y\frac{\partial}{\partial x}$.

As usual we take X to be at least of class C^∞ ; we recall that such a singularity is called a nilpotent singularity or nilpotent singular point.

Using the Formal Normal Form Theorem presented in Sect. 2.1 and, more specifically, the example treated there, we find the following normal form for C^∞ -conjugacy:

$$\begin{aligned}\dot{x} &= y + A(x, y), \\ \dot{y} &= f(x) + yg(x) + y^2B(x, y),\end{aligned}$$

where f , g , A , and B are C^∞ functions, $j_1f(0) = g(0) = j_\infty A(0, 0) = j_\infty B(0, 0) = 0$. By introducing the new variable $Y = y + A(x, y)$, we change the former expression into

$$\begin{aligned}\dot{x} &= y, \\ \dot{y} &= f(x) + yg(x) + y^2B(x, y),\end{aligned}\tag{3.6}$$

for appropriately adapted f , g , and B with similar properties as before. If $B \equiv 0$, then the system comes from the Liénard equation $\ddot{x} = f(x) + \dot{x}g(x)$. We now make a complete local topological study of all cases in which $j_\infty f(0)$ is not zero. This includes the local study of the related Liénard equations. Either $j_\infty g(0) \neq 0$ and

$$\begin{aligned}f(x) &= ax^m + o(x^m), \\ g(x) &= bx^n + o(x^n),\end{aligned}\tag{3.7}$$

with $ab \neq 0$, or $j_\infty g(0) = 0$. The dual 1-form of (3.6) is given by

$$-ydy + (f(x) + yg(x) + y^2B(x, y))dx,$$

which is equal to

$$-ydy + d\bar{f}(x) + yd\bar{g}(x) + y^2B(x, y)dx,\tag{3.8}$$

for some C^∞ functions \bar{f} and \bar{g} such that

$$\begin{aligned}\bar{f}(x) &= \frac{ax^{m+1}}{m+1} + o(x^{m+1}) \quad \text{and} \\ \bar{g}(x) &= \frac{bx^{n+1}}{n+1} + o(x^{n+1}),\end{aligned}$$

provided $j_\infty g(0) \neq 0$.

A linear change in x permits \bar{f} to be changed into

$$\bar{f}(x) = \frac{\delta x^{m+1}}{m+1} + o(x^{m+1}),$$

with $\delta = 1$ in case m is even and $\delta = \pm 1$ in case m is odd. Changing y by $-y$ if necessary we may suppose that $b > 0$. Instead of reducing a to δ , we could also perform on \bar{g} an operation similar to the one performed on \bar{f} to reduce b to $+1$, hence obtaining

$$\bar{g}(x) = \frac{x^{n+1}}{n+1} + o(x^{n+1}),$$

provided $j_\infty g(0) \neq 0$.

So up to linear (not necessarily orientation preserving) equivalence, we can suppose that in expression (3.7)

$$\text{either } a = \delta \text{ and } b > 0, \text{ or } b = 1, \quad (3.9)$$

with $\delta = 1$ when m is even and $\delta = \pm 1$ when m is odd.

If $j_\infty g(0) \neq 0$, we observe that a coordinate change

$$y = Y + \int_0^x g(u) du = Y + G(x), \quad (3.10)$$

permits changing an expression (3.6) with $B \equiv 0$ into

$$\begin{aligned} \dot{x} &= Y + G(x), \\ \dot{y} &= f(x). \end{aligned}$$

If $B \neq 0$, then (3.10) changes expression (3.6) into

$$\begin{aligned} \dot{x} &= Y + G(x), \\ \dot{Y} &= F(x) + YH(x) + Y^2D(x, Y), \end{aligned} \quad (3.11)$$

where G , F , H , and D are C^∞ functions, $j_\infty F(0) = j_\infty f(0)$, $j_\infty H(0) = j_\infty D(0, 0) = 0$. By a well chosen C^∞ coordinate change $Y = y + \alpha(x)$ with $j_\infty \alpha(0) = 0$ we can even change (3.11) into

$$\begin{aligned} \dot{x} &= y + \bar{G}(x), \\ \dot{y} &= \bar{F}(x) + y^2 C(x, y), \end{aligned} \quad (3.12)$$

with $j_\infty \bar{G}(0) = j_\infty G(0)$, $j_\infty \bar{F}(0) = j_\infty F(0)$ and $j_\infty C(0, 0) = 0$. Then expression (3.12) is also valid if $j_\infty g(0) = 0$.

We write (3.12) as

$$\begin{aligned} \dot{x} &= y + H(x), \\ \dot{y} &= F(x) + y^2 C(x, y), \end{aligned} \quad (3.13)$$

with $H(0) = 0$. The relation between (3.12) and (3.13) is given by

$$\begin{aligned} j_\infty H'(0) &= j_\infty g(0), \\ j_\infty F(0) &= j_\infty f(0). \end{aligned}$$

The study of these singularities now relies on (quasihomogeneous) blow-up. We systematically work it out, depending on the values of m and n , where $m \geq 2$ and $n \geq 1$ including $n = \infty$, the latter of which means that we accept $j_\infty g(0) = 0$ in expression (3.6).

We distinguish three cases.

Hamiltonian like case: $m < 2n + 1$. If m is odd we use the blow-up

$$x = u, \quad y = u^k \bar{y}, \tag{3.14}$$

with $k = (m + 1)/2$ and we divide by u^{k-1} .

If m is even we use

$$x = u^2, \quad y = u^{m+1} \bar{y}, \tag{3.15}$$

and we divide by u^{m-1} .

Singular like case: $m > 2n + 1$. We use the blow-up

$$x = u, \quad y = u^{n+1} \bar{y}, \tag{3.16}$$

and we divide by u^n .

Mixed case: $m = 2n + 1$. We use again the blow-up (3.16)

In all cases there is no need to check the directional charts $\{\bar{y} = \pm 1\}$ because of the specific expression of the linear part. We may also restrict to $\{\bar{x} = 1\}$, since the n -exponent in front of \bar{x} is odd, except for blow-up (3.15).

3.4.1 Hamiltonian Like Case ($m < 2n + 1$)

We start with expression (3.8) for the dual 1-form and change $\bar{f}(x)$ to $\delta x^{m+1}/(m+1)$ by a coordinate change in x . This changes expression (3.6) by C^∞ equivalence into

$$\begin{aligned} \dot{x} &= y, \\ \dot{y} &= \delta x^m + y(bx^n + o(x^n)) + O(y^2). \end{aligned}$$

Case m odd: We know that $\delta = \pm 1$ and we use blow-up (3.14) in the \bar{x} -direction $(x, y) \mapsto (u, u^k \bar{y})$, with $k = (m + 1)/2$. After division by u^{k-1} we get

$$\begin{aligned} \dot{u} &= u \bar{y}, \\ \dot{\bar{y}} &= (\delta - k \bar{y}^2) + O(u). \end{aligned}$$

The blow-up and related phase portraits for this system that can be seen in Fig. 3.13.

For $\delta = 1$ we get a singularity of saddle-type. One can prove that it is C^0 -conjugate to a hyperbolic saddle, but we will not work it out, as announced before. The contact between the different separatrices is described by the blowing up mapping.

For $\delta = -1$ we get a singularity of center or focus type. It is not a simple problem to determine whether it is a center or a focus.

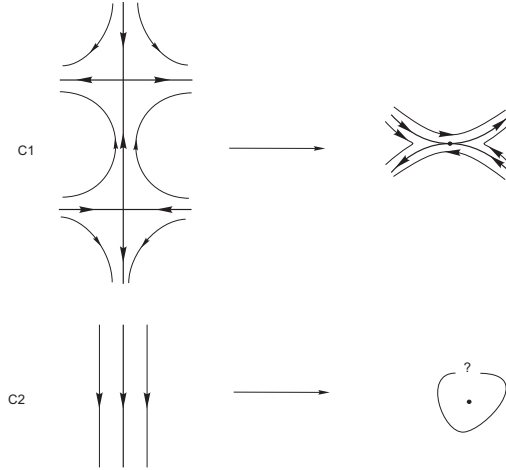


Fig. 3.13. Desingularization of Hamiltonian like case when m is odd

Case m even: In this case we can take $\delta = 1$ and we use blow-up (3.15) in the \bar{x} -direction as well as in the $-\bar{x}$ -direction

$$(x, y) = (u^2, u^{m+1}\bar{y}), \quad \text{or}$$

$$(x, y) = (-u^2, u^{m+1}\bar{y}).$$

After division by u^{m-1} we get, respectively,

$$\dot{u} = \frac{u\bar{y}}{2}, \quad \text{and} \quad \dot{u} = -\frac{u\bar{y}}{2},$$

$$\dot{\bar{y}} = \left(1 - \frac{m+1}{2}\bar{y}^2\right) + O(u), \quad \text{and} \quad \dot{\bar{y}} = \left(1 + \frac{m+1}{2}\bar{y}^2\right) + O(u).$$

The blow-up and related phase portraits for this system can be seen in Fig. 3.14.

We get a singularity consisting of two hyperbolic sectors. It is called a *cusp point*. The contact between the separatrices is described by the blowing up mapping.

We note that in the Hamiltonian like case we can also take $n = +\infty$, meaning that $j_\infty g(0) = 0$ in expression (3.6).

3.4.2 Singular Like Case ($m > 2n + 1$)

We start with expression (3.8) for the dual 1-form and, making analogous changes as in the Hamiltonian like case but on \bar{g} instead of \bar{f} , we change expression (3.6) by C^∞ equivalence, and possible time reversion, into

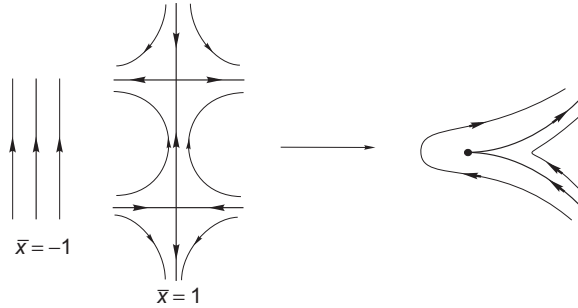


Fig. 3.14. Desingularization of Hamiltonian like case when m even

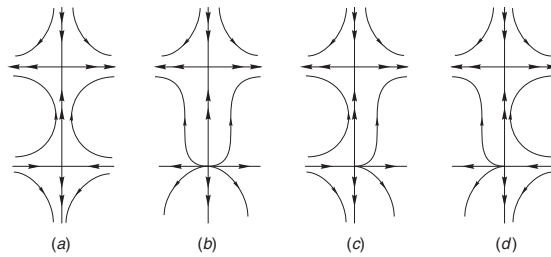


Fig. 3.15. Blow-ups of the singular like case

$$\begin{aligned} \dot{x} &= y, \\ \dot{y} &= ax^m + y(x^n + o(x^n)) + O(y^2), \end{aligned}$$

with $a \neq 0$.

We use blow-up (3.16) in the \bar{x} -direction

$$(x, y) = (u, u^{n+1}\bar{y}).$$

After division by u^n we get

$$\begin{aligned} \dot{u} &= u\bar{y}, \\ \dot{\bar{y}} &= \bar{y}(1 - (n + 1)\bar{y}) + O(u) + au^{m-2n-1}. \end{aligned}$$

On $\{u = 0\}$ we find two singularities, situated, respectively, at $\bar{y} = 1/(n + 1)$ and at $\bar{y} = 0$. The former is clearly a hyperbolic saddle. The latter is a semi-hyperbolic point with $\{u = 0\}$ as unstable manifold and having a center manifold transverse to it. We leave it as an exercise to prove that the center behavior is not flat, because of the presence of the term au^{m-2n-1} . This leads to the possible portraits for the blow-up given in Fig. 3.15.

In getting the $\{\bar{x} = -1\}$ -chart out of these pictures, we must take care concerning the parity of n . Depending on the parity of n , cases (b) and (d) in Fig. 3.15 will induce two different phase portraits (see, respectively, (a), (c) and (e), (f) in Fig. 3.16).

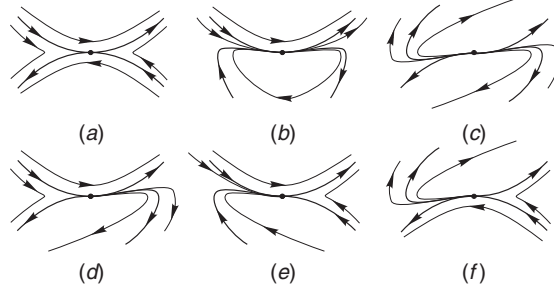


Fig. 3.16. Phase portraits of the singular like case

The totality of phase portraits obtained is represented in Fig. 3.16. Again the contact in between the separatrices is clear from the blow-up mapping.

The cases (d) and (f) are topologically equivalent, so we have five different phase portraits.

Figure 3.16 may give the impression that a global attractor, similar to the global repeller in (c), might not be possible in the singular like case, but this is merely because of the choice of the coefficients in the normal form. Multiplying the vector field by -1 , corresponding to a time reversal, creates the possibility of getting such an attractor. Thus there are six topologically distinct phase portraits in all.

3.4.3 Mixed Case ($m = 2n + 1$)

We start with expression (3.8) for the dual 1-form and, making analogous changes as in the previous cases, we change expression (3.6) by C^∞ equivalence, and possible time reversion, into

$$\begin{aligned} \dot{x} &= y, \\ \dot{y} &= ax^{2n+1} + y(x^n + o(x^n)) + O(y^2), \end{aligned}$$

with $a \neq 0$.

We use blow-up (3.16) in the \bar{x} -direction $(x, y) = (u, u^{n+1}\bar{y})$. After division by u^n we get

$$\begin{aligned} \dot{u} &= u\bar{y}, \\ \dot{\bar{y}} &= a + \bar{y} - (n + 1)\bar{y}^2 + \bar{y}O(u), \end{aligned}$$

with $a \neq 0$.

On $\{u = 0\}$ the singularities are given by the solution of

$$a + \bar{y} - (n + 1)\bar{y}^2 = 0.$$

We either have zero, one, or two solutions. No solution can be situated at the origin, since $a \neq 0$. The blow-ups are shown in Fig. 3.17.

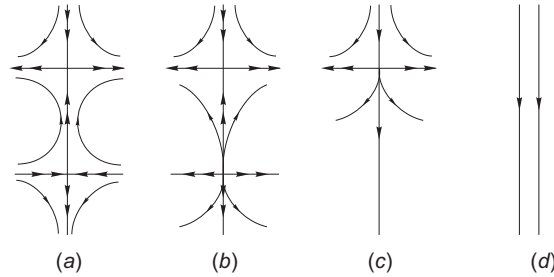


Fig. 3.17. Blow-ups of the mixed case

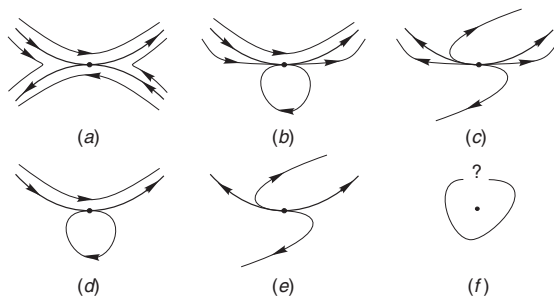


Fig. 3.18. Phase portraits of the mixed case

Again, depending on the parity of n , cases (b) and (c) give rise to two different phase portraits.

The blow-ups in Fig. 3.17 hence induce the phase portraits of Fig. 3.18.

Although contacts of separatrices might differ, these phase portraits are not topologically different from the ones we already found before. In case (f) we are again left with a center or focus problem.

Remark 3.4 One can prove that for nilpotent singularities with $j_\infty f(0) \neq 0$, there are eight different classes for topological conjugacy. As we have seen, the multiplicity is clearly given by the number m .

With respect to (3.6) it remains to consider the cases in which $j_\infty f(0) = 0$.

We perform this study only for analytic vector fields. We start with an analytic vector field X given by

$$\begin{aligned} \dot{x} &= y + \alpha(x, y), \\ \dot{y} &= \beta(x, y), \end{aligned}$$

with α and β analytic, $j_1\alpha(0, 0) = j_1\beta(0, 0) = 0$.

If we introduce the new variable $Y = y + \alpha(x, y)$, and write y instead of Y , then we get

$$\begin{aligned} \dot{x} &= y, \\ \dot{y} &= \delta(x) + y\gamma(x, y). \end{aligned} \tag{3.17}$$

We now prove that

$$j_\infty f(0) = 0 \quad \text{if and only if} \quad \delta(x) \equiv 0. \quad (3.18)$$

The Normal Form Theorem relies on transformations of the form

$$(u, v) = (x + A(x, y), y + B(x, y)), \quad (3.19)$$

with A and B polynomials of a given degree n ; the procedure uses an induction on n . To prove (3.18) we need only make a formal calculation, that is simply look at ∞ -jets at $(0, 0)$. The operation to transform (3.17) to a normal form by means of (3.19) implies that

$$\begin{aligned} \left(1 + \frac{\partial A}{\partial x}\right) y + \frac{\partial A}{\partial y} (\delta(x) + y\gamma(x, y)) &= y + B(x, y), \\ \frac{\partial B}{\partial x} y + \left(1 + \frac{\partial B}{\partial y}\right) (\delta(x) + y\gamma(x, y)) &= f(x + A(x, y)) \\ &\quad + (y + B(x, y))\Gamma(x, y), \end{aligned} \quad (3.20)$$

for some function Γ .

If we consider the second equation at $y = 0$, this gives

$$\left(1 + \frac{\partial B}{\partial y}(x, 0)\right) \delta(x) = f(x + A(x, 0)) + B(x, 0)\Gamma(x, 0).$$

Taking into account the degree of the terms, we see that $j_n \delta(0) = j_n f(0)$ when $j_{n-1} \delta(0) = j_{n-1} f(0) = 0$.

An induction argument hence shows that both f and δ have the same term of lowest degree, with the same coefficient.

Therefore the condition $j_\infty f(0) = 0$ on the normal form implies that $\delta(x) \equiv 0$ in expression (3.17), and we get the vector field X given by

$$\begin{aligned} \dot{x} &= y, \\ \dot{y} &= y\gamma(x, y), \end{aligned} \quad (3.21)$$

for which $\{y = 0\}$ is a line of singularities.

We now prove that

$$j_\infty g(0) = 0 \quad \text{if and only if} \quad \gamma(x, 0) = 0. \quad (3.22)$$

This means that, under the condition $j_\infty f(0) = 0$, $j_\infty g(0) = 0$ as well if and only if the divergence of X is identically zero along the curve of singularities.

The proof of (3.22) is similar to the proof of (3.18). Instead of (3.20) we now find the equations (at the ∞ -jet level)

$$\begin{aligned} \left(1 + \frac{\partial A}{\partial x}\right) y + \frac{\partial A}{\partial y} y\gamma(x, y) &= y + B(x, y), \\ \frac{\partial B}{\partial x} y + \left(1 + \frac{\partial B}{\partial y}\right) y\gamma(x, y) &= (y + B(x, y))g(x + A(x, y)). \end{aligned}$$

In the second equation we see that

$$B(x, 0)g(x + A(x, 0))$$

has to be zero. So either $B(x, 0) = 0$ or $j_\infty g(0) = 0$.

We first take $B(x, 0) = 0$. If we now divide the second equation by y , and put $y = 0$ we then get

$$\left(1 + \frac{\partial B}{\partial y}(x, 0)\right) \gamma(x, 0) = g(x + A(x, 0)),$$

implying that the n -jet of $\gamma(x, 0)$ is given by $j_n g(0)$ when their $(n - 1)$ -jets are both zero. If however $j_\infty g(0) = 0$, then we get

$$\frac{\partial B}{\partial x}(x, 0) + \left(1 + \frac{\partial B}{\partial y}(x, 0)\right) \gamma(x, 0) = 0,$$

implying inductively that the ∞ -jet of $\gamma(x, 0)$ also has to be zero.

We hence find two different situations for expressions (3.21). On the one hand we have

$$\begin{aligned} \dot{x} &= y, \\ \dot{y} &= y^2 \varphi(x, y), \end{aligned} \tag{3.23}$$

describing the cases whose formal normal form is zero. The phase portrait is obtained by drawing the flow box

$$\begin{aligned} \dot{x} &= 1, \\ \dot{y} &= y \varphi(x, y), \end{aligned}$$

and multiplying it by the function y . The result is presented in Fig. 3.19.

On the other hand we have the analytic expressions

$$\begin{aligned} \dot{x} &= y, \\ \dot{y} &= yx^n(1 + r(x)) + y^2 \psi(x, y), \end{aligned} \tag{3.24}$$

for some $n \geq 1$.

It is again a flow box multiplied by the function y . The flow box is

$$\begin{aligned} \dot{x} &= 1, \\ \dot{y} &= x^n(1 + r(x)) + y \psi(x, y). \end{aligned} \tag{3.25}$$

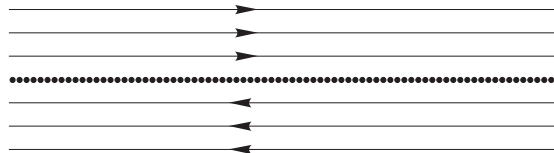


Fig. 3.19. Phase portrait of (3.23)

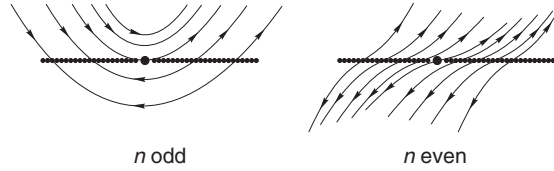


Fig. 3.20. Phase portrait of (3.24)

Along $\{y = 0\}$ the contact of (3.25) with the x -axis is described by

$$\dot{y} = x^n(1 + r(x)) \sim x^n.$$

This leads to the phase portraits described in Fig. 3.20.

3.5 Summary on Nilpotent Singularities

Here we give a specific and practical theorem which summarizes the previous results and which is very helpful for determining the local behavior at a nilpotent singular point; see [2] for more details.

Theorem 3.5 (Nilpotent Singular Points Theorem) *Let $(0, 0)$ be an isolated singular point of the vector field X given by*

$$\begin{aligned} \dot{x} &= y + A(x, y), \\ \dot{y} &= B(x, y), \end{aligned} \tag{3.26}$$

where A and B are analytic in a neighborhood of the point $(0, 0)$ and also $j_1A(0, 0) = j_1B(0, 0) = 0$. Let $y = f(x)$ be the solution of the equation $y + A(x, y) = 0$ in a neighborhood of the point $(0, 0)$, and consider $F(x) = B(x, f(x))$ and $G(x) = (\partial A/\partial x + \partial B/\partial y)(x, f(x))$. Then the following holds:

- (1) If $F(x) \equiv G(x) \equiv 0$, then the phase portrait of X is given by Fig. 3.21a.
- (2) If $F(x) \equiv 0$ and $G(x) = bx^n + o(x^n)$ for $n \in \mathbb{N}$ with $n \geq 1$ and $b \neq 0$, then the phase portrait of X is given by Fig. 3.21b or c.
- (3) If $G(x) \equiv 0$ and $F(x) = ax^m + o(x^m)$ for $m \in \mathbb{N}$ with $m \geq 1$ and $a \neq 0$, then
 - (i) If m is odd and $a > 0$, then the origin of X is a saddle (see Fig. 3.21d) and if $a < 0$, then it is a center or a focus (see Fig. 3.21e–g);
 - (ii) If m is even then the origin of X is a cusp as in Fig. 3.21h.
- (4) If $F(x) = ax^m + o(x^m)$ and $G(x) = bx^n + o(x^n)$ with $m \in \mathbb{N}$, $m \geq 2$, $n \in \mathbb{N}$, $n \geq 1$, $a \neq 0$ and $b \neq 0$, then we have
 - (i) If m is even, and
 - (i1) $m < 2n + 1$, then the origin of X is a cusp as in Fig. 3.21h;

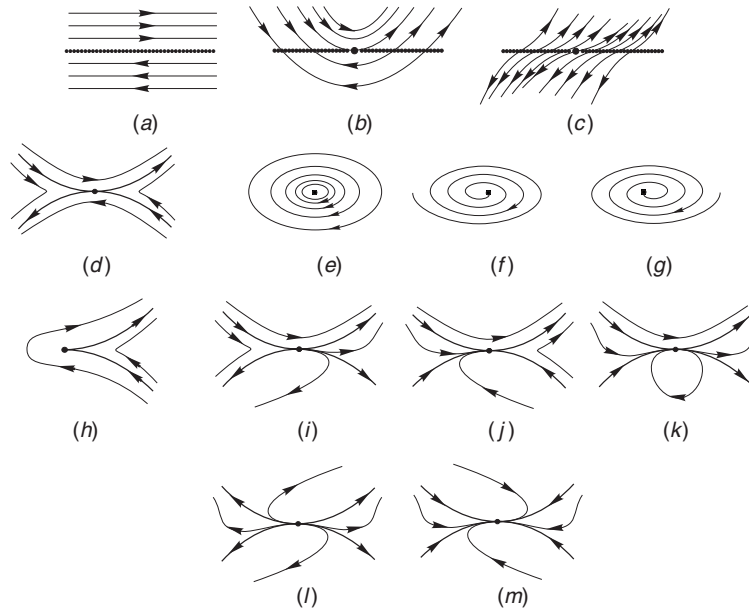


Fig. 3.21. Phase portraits of nilpotent singular points

- (i2) $m > 2n + 1$, then the origin of X is a saddle-node as in Fig. 3.21i or j;
- (ii) If m is odd and $a > 0$ then the origin of X is a saddle as in Fig. 3.21d;
- (iii) If m is odd, $a < 0$ and
 - (iii1) Either $m < 2n + 1$, or $m = 2n + 1$ and $b^2 + 4a(n + 1) < 0$, then the origin of X is a center or a focus (see Fig. 3.21e-g);
 - (iii2) n is odd and either $m > 2n + 1$, or $m = 2n + 1$ and $b^2 + 4a(n + 1) \geq 0$, then the phase portrait of the origin of X consists of one hyperbolic and one elliptic sector as in Fig. 3.21k;
 - (iii3) n is even and either $m > 2n + 1$, or $m = 2n + 1$ and $b^2 + 4a(n + 1) \geq 0$, then the origin of X is a node as in Fig. 3.21l, m. The node is attracting if $b < 0$ and repelling if $b > 0$.

Remark 3.6 In Fig. 3.21 we have represented all possible phase portraits of nilpotent singularities. In the pictures we have paid attention to the fact that the separatrices have certain contacts, but we have of course not stressed the exact order of contact they have. This easily follows from the blow-up procedures. We have also ignored to the exact position of the different separatrices in relation to $\{y = 0\}$ in case that we change the expression of (3.26), by means of an analytic coordinate change, to a new one in which $x = y$. Such information can also be easily been obtained by the blow-up procedure.

Remark 3.7 Section 3.4 has not really been arranged in such a way as to contain a systematic proof of this theorem. We have preferred to treat the different nilpotent singularities according to the kind of blow-up that is needed to study them. It is however clear that in order to get a precise proof of Theorem 3.5 it is sufficient to go through the different cases and to apply the blow-ups as indicated in Sect. 3.4. We can leave this as an exercise.

The remaining center-focus problem, on the other hand, is an open problem.

3.6 Exercises

Exercise 3.1 Consider the vector field $(y + 2x^3)\frac{\partial}{\partial x} + (x^2 + xy + y^3)\frac{\partial}{\partial y}$. Make an appropriate quasihomogeneous blow-up at the origin and calculate a parametrization $\gamma : (\mathbb{R}, 0) \rightarrow (\mathbb{R}^2, 0)$ of the two separatrices, up to terms of order 5, i.e., with a remainder of order $O(t^5)$.

Exercise 3.2 Study the following vector fields by means of an appropriate quasihomogeneous blow-up

- (i) $-y\frac{\partial}{\partial x} + x^3\frac{\partial}{\partial y}$,
- (ii) $(y^3 + xy^2)\frac{\partial}{\partial x} + x^2\frac{\partial}{\partial y}$.

Exercise 3.3 Let X be a C^∞ vector field satisfying a Lojasiewicz inequality at p and suppose that the C^∞ vector field Y at q is C^∞ -conjugate to X at p . Show that Y at q also satisfies a Lojasiewicz inequality.

Exercise 3.4 Check that the following vector fields satisfy a Lojasiewicz inequality at the origin:

- (i) $(y + x^3)\frac{\partial}{\partial x} - x^3\frac{\partial}{\partial y}$.
- (ii) $(x + y)\frac{\partial}{\partial x} + y^4\frac{\partial}{\partial y}$.

Exercise 3.5 Prove that a Lojasiewicz inequality holds for

- (i) all hyperbolic singularities.
- (ii) Singularities whose 1-jet is a center.
- (iii) Semi-hyperbolic singularities with nonflat center behavior.
- (iv) Nilpotent singularities for which in (3.6) $j_\infty f(0) \neq 0$ holds.

Exercise 3.6 Prove that a C^∞ vector field X satisfies a Lojasiewicz inequality at a singularity p if and only if there exists a finite jet $j_k X(p)$ with the property that $\|j_k X(p)\| \geq c\|x\|^k$ for some $c > 0$.

Exercise 3.7 Prove that no Lojasiewicz inequality holds for the vector field

$$X = (y + x^2)^2 \frac{\partial}{\partial x} + (y + x^2) \frac{\partial}{\partial y},$$

but its 2-jet $j_2X(0)$ does satisfy a Lojasiewicz inequality $\|j_2X(0)\| \geq c\|x\|^4$ for some $c > 0$.

Exercise 3.8 Prove the existence of a finite sectorial decomposition for the following singularities at $(0, 0)$.

- (i) $y \frac{\partial}{\partial x} + x^2 \frac{\partial}{\partial y}$,
- (ii) $(3x^2 - 2xy) \frac{\partial}{\partial x} + (y^2 - 3xy) \frac{\partial}{\partial y}$,
- (iii) $(x^2 - y^2) \frac{\partial}{\partial x} + 2xy \frac{\partial}{\partial y}$,
- (iv) $x^2 \frac{\partial}{\partial x} + y(2x - y) \frac{\partial}{\partial y}$

Exercise 3.9 Consider the vector field in Example 3.1, of which the local phase portrait is represented in Fig. 3.2,

$$X = (x^2 - 2xy) \frac{\partial}{\partial x} + (y^2 - xy) \frac{\partial}{\partial y} + O(\|(x, y)\|^3).$$

- (i) Show that for ε sufficiently small, the six separatrices of this system cut $S_\varepsilon = \{(x, y) | x^2 + y^2 = \varepsilon\}$ transversely.
- (ii) Show that for each of these systems the “finite sectorial decomposition” property holds on some neighborhood V of the origin.
- (iii) Prove that any two of the above systems are locally C^0 -equivalent.
- (iv) Show that inside any hyperbolic sector, the time to go from the boundary ∂V to itself tends monotonically to infinity when the orbit approaches the separatrices.
- (v) Use (iv) to prove that any two of the above systems are mutually C^0 -conjugate.

Exercise 3.10 Show that for any C^∞ singularity of Lojasiewicz type (satisfying a Lojasiewicz inequality) with a characteristic orbit, there is a finite sectorial decomposition whose boundary is C^∞ .

Remark: The proof of the existence of a C^∞ boundary relies on the use of a “ C^∞ -partition of the unity.” As a first step in the proof we suggest proving the existence of a C^0 boundary.

Exercise 3.11 Check that every C^∞ singularity that satisfies a Lojasiewicz inequality but does not have a characteristic orbit is necessarily monodromic.

Hint: Provide a proof based on the theorems that are cited in the book, even those whose proof is not incorporated.

Exercise 3.12 Use Theorem 3.5 to check the nature of the singularity at the origin of

$$(-x^2 + ay^2 - xy - 2xy^2) \frac{\partial}{\partial x} + (y^2 + xy + y^3) \frac{\partial}{\partial y},$$

with $a \neq 0$ and $1 + 2a > 0$.

3.7 Bibliographical Comments

The desingularization theorem for planar vector fields has a long history. It was first stated by Bendixson in 1901, however without proof. The paper also included the topological classification of the elementary singular points.

In 1968, Seidenberg gave the first rigorous proof of the theorem for the analytic case. The desingularization procedure was extended to C^∞ vector fields of Lojasiewicz type in [52]. This paper is based on the Ph.D.-thesis of Dumortier from 1973. In the mid seventies, van den Essen found a transformed proof of the desingularization theorem for analytic vector fields; see [159].

In all previous papers, the desingularization was based on quadratic transformations, or in the real case, on polar blow-up, hence in the terminology of this chapter, on the homogeneous blow-up.

Quasihomogeneous blow-up was already used in the book of Lyapunov [106] but was essentially put forward as a systematic and a more powerful technique in the paper by Brunella and Miari [22] and especially in the book of Bruno [23]. A proof of the desingularization theorem for C^∞ vector fields of Lojasiewicz type, based on quasihomogeneous blow-ups, was given by Pelletier in her thesis [124]; see also [125]. The desingularization procedure used in the program P4 [9] is based on the algorithm presented in that thesis. The classification of nilpotent singularities can be found in the papers of Andreev [2] and of Arrowsmith [8]. The elaboration that we provide in this chapter is based on quasihomogeneous blow-up and is by far the simplest that seems possible.